ISSN: 2688-8653

Experimental Study on Flexural Behavior of Cold-formed Thin-wall C-section Spliced Beams

Bingyang Yang[1], Xiuyan Fu[1, 2, *], Cao Xu[1], Jiangming Tang[3]

[1]Institute of Civil Engineering, North China University of Science and Technology, Tangshan 063210, China

[2]Earthquake Engineering Research Center of HeBei Province, Tangshan 063210, China

[3]Handan Construction Engineering Group Co, LTD, Handan, 056001, China

*fuxiuyan@ncst.edu.cn

Abstract

The flexural properties of four test members and the finite element simulation of four test members are carried out for the double limb spliced large section cold formed thin-wall steel beam,The failure modes, ultimate bearing capacity and displacement ductility coefficient of each specimen were obtained by controlling the influence of the spacing of tapping screws and different assembling modes on the components. The results show that: The mechanical properties of beams with 150mm screw spacing are slightly better than those with 300mm screw spacing.The bending bearing capacity of i-shaped beams is significantly better than that of box-shaped beams, and the ultimate bearing capacity is increased by about 30%.In each group of specimens test and numerical calculation results analysis,the ductility of box girder is slightly better than that of I-beam, and the spacing of tapping screws has little effect on the ductility of large section cold formed thin-walled steel girder.

Keywords

Large Section Cold Formed Thin Wall Steel; Double-Limb Spliced I-Beam; Double Limb Split Box Beam; Bending Capacity; Displacement Ductility Coefficient.

1. The Introduction

Cold-formed Steel[1](cold-formed Steel[2]) is generally made of hot-rolled or cold-rolled Steel as raw material, which can be bent into various section shapes by drawing, stamping, bending or roller bending forming units at normal temperature.Cold-formed thin-wall steel is made of steel plate or strip with thickness of 1.5~6mm by cold processing.The thickness of the same section is the same, and the corners of the section are rounded.In the construction, often use all kinds of roof truss, diamond frame, net frame, purlin, wall beam, wall column and other structures and components made of thin-wall steel.However, the yield point of cold-formed section steel increases obviously due to cold-working hardening, which has a good influence on the mechanical characteristics of the structure, so a lot of steel can be saved.The cold-formed thin-wall steel component is light in volume, versatile, easy to be made in industry, and can be reused.It is a building component with great space for future development, and makes a great contribution to the green construction advocated by China.Due to the rapid development of cold-formed thin-wall processing technology, now cold-formed thin-wall steel has been more used in various fields, such as vehicles, aircraft, light industry, construction and so on.Especially in the field of engineering application, cold-formed thin-wall steel is favored by the industry because of its many advantages.In China, the research on double spliced cold-formed thin-walled beams started late, but a lot of research has been done in recent years.Wu Sheng et al.[3-

ISSN: 2688-8653

4] conducted finite element simulation analysis on welding connections made of ∑components.The results show that the flexural capacity of the segmented section member is significantly higher than that of the single-limb ∑member, and the deformation of the member is small without distortion buckling.Zhou Xuhong et al.[5-7]analyzed and studied the flexural performance of double spliced cold-formed thin-walled I-steel beams by combining test and finite element analysis, taking material strength, opening holes on test members, width-thickness ratio of flanges, width-thickness ratio of webs and plate thickness as changing parameters.The effective width method[8]and reduction strength method[9]are proposed to calculate the properties of cold-formed thin-wall steel in China.At present, there are few literatures on the flexural properties of cold-formed thin-walled C-section spliced-beams in China [10], and the applicability of direct strength method in such spliced-beams needs to be systematically tested and analyzed.

2. Theoretical Equation

In order to be more convenient in the design calculation,in the traditional effective width method,the ultimate bearing capacity of the plate is dedtermined by using therectangular effctive area with the maximum edge stress $b_e/2$ as the unique factor go to lciba to see more,approach:

$$P_u = tb_e f_y = A_e f_y$$

For the above formula,there is only one unknown parameter,so the limitbearing capacity of the component b_e can be calculated as long as the values aredeterniber,Winter obtained semi-theoretical formulas for the effectivewidth through extensive experiments as well as data analysis:

$$b_e = \rho b$$

in the formula:

$$\rho = \sqrt{\frac{f_{ol}}{F_n}}\left[1 - 0.22\sqrt{\frac{f_{ol}}{F_n}}\right]$$

f_{ol} -elastic local buckling stress of plate

F_n -maximum stress at plate edge

Formulas for calculating the direct strength of axial compression and bending members:

Axial compression artifacts:

When $\lambda_d \leq 0.561$:

$$P_d = P_y = Af_y$$

When $\lambda_d > 0.561$:

$$P_d = \left[1 - 0.25\left(\frac{P_{crd}}{P_y}\right)^{0.6}\right]\left(\frac{P_{crd}}{P_y}\right)^{0.6} P_y$$

For bending members,parameters $\lambda_d = \sqrt{M_y/M_{crd}}$

When: $\lambda_d \leq 0.561$:

$$M_d = M_y = W_x f_y$$

ISSN: 2688-8653

When: $\lambda_d > 0.561$:

$$M_d = \left[1 - 0.22\left(\frac{P_{crd}}{P_y}\right)^{0.5}\right]\left(\frac{P_{crd}}{P_y}\right)^{0.5} M_y$$

The theoretical bearing capacity of each test component is calculated by substituting the basic data of the test component:

III-A: MAmax=20.5kN·m FAmax=34.1kN

III-B: MBmax=19.97kN·m FBmax=33.82kN

III-C: MCmax2=13.99kN·m FCmax=21.76kN

III-D: MDmax2=13.86kN·m FDmax=21.43kN

3. Test Design

3.1. Specimen Design

The sectional sections of this study are all composed of C300×50×8×1.5 size basic members pieced together at a certain distance by ST4.8 tapping and self-drilling screws.The theoretical section of the basic test members is shown in Figure 1.The same cold-formed thin-walled C-section steel was used to assemble different sections.A total of four groups of test members were used to analyze the bending capacity of cold-formed thin-walled steel beams by studying different assembling methods and screw spacing.Specimens A and B used box assembling method with screw spacing of 150mm and 300mm.Specimens C and D adopt i-splicing mode, and screw spacing is 150mm and 300mm respectively.In order to prevent local buckling at the loading point and support in the test, the loading point at 1/3 of the span on both sides and the positions at both ends of the support are respectively set with stiffeners of model C89×41×2×1.5.The specific parameters of the components are shown in Table 1.

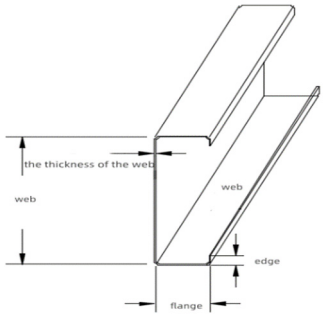

Figure 1. Test component section form

Table 1. Parameters of test components

Test component number	Section /mm	Screws pacings /mm	Initial imperfection ξ_{max}/mm	Length of test member
III-A	C300×50×8×1.5×2	150	0.19	2100
III-B	C300×50×8×1.5×2	300	0.23	2100
III-C	C300×50×8×1.5×2	150	0.25	2100
III-D	C300×50×8×1.5×2	300	0.22	2100

ISSN: 2688-8653

3.2. Material Mechanical Properties Test

In order to improve the accuracy of test components and avoid damaging test compo-nents and causing test errors, the method of laser cutting is selected to cut test comp-onents P1, P2 and P3 from the steel strip, as shown in Figure 2.

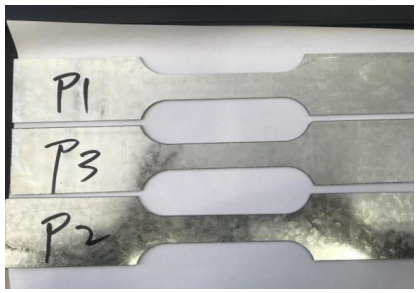

Figure 2. Laser cut specimen

Table 2. Main test results of material properties test

specimen number	the thickness of the material (t/mm)	the yield strength (fy/Mpa)	tensile strength (fu/Mpa)	elongation (σ/%)	modulus of elasticity (E/105Mpa)
P1	1.48	325.02	363.12	16.21%	2.03
P2	1.49	316.13	361.33	16.32%	2.05
P3	1.51	329.42	364.21	16.03%	1.98
The average	1.49	323.52	362.89	16.19%	2.02

3.3. Layout of Test Device and Measuring Point

The production of the test beam uses a set of fixtures to fix the test member, to limit the lateral displacement of the test member to prevent the lateral instability of the member in the loading process, this method is also more real simulation of the actual situation of secondary beam wall and floor constraints on the beam.

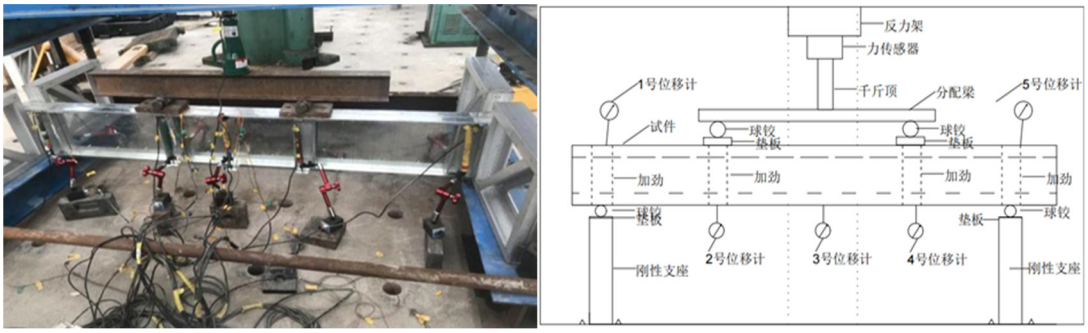

(a) Loading device site (b) Schematic diagram of loading device

Figure 3. Test loading device

ISSN: 2688-8653

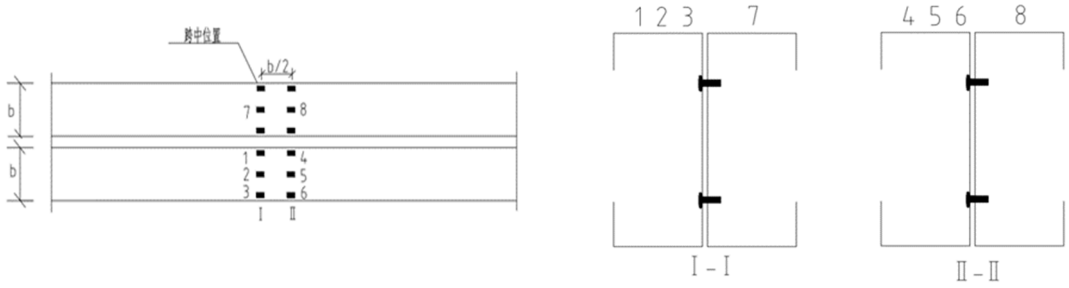

(a) Plane position of strain gauge layout (b) Position of strain gauge layout profile

Figure 4. Strain gauge layout of I-shaped test member

4. Loading System

Before the test, the bending capacity of single cold-formed thin-wall C-section steel was calculated according to the Technical Code for Cold-formed Thin-wall Steel Structures (GB50018-2002), and the ultimate bearing capacity of test members was estimated by superposition. Before the test, the test components are aligned, and 20% of the estimated load is applied in advance as the pre-loading load, so that the gaps of the components are closer because of the residual during the pre-production. During loading, 5% of the estimated load was used as the loading load of each stage, and the loading was suspended for 2min after the completion of each stage to observe the changes of the test components. When the loading load reaches 80% of the estimated load, the loading range is reduced until the component deforms greatly and the bearing capacity does not rise any more, which means that the component is damaged. When the loading capacity continues to decrease gradually and decreases to 85% of the estimated load, the loading stops.All data in the test are collected by the data collector.

5. Test Results and Analysis

5.1. Experimental Phenomenon and Damage Form

When the box fitting test components were destroyed, the webs were slightly bulged, and the support webs were concave inward. Finally, due to local buckling of the webs, the bearing capacity of the components was lost. Local damage is shown in Figure 5.

With the increasing load of i-shaped split-beam, first the web began to bend, then the tapping screws at one third of the support were individually cut, and finally the web at the support local buckling, and finally lost the bearing capacity. Local damage is shown in Figure 6.

Figure 5. Local buckling failure of box girder

ISSN: 2688-8653

Figure 6. Local buckling failure of I-shaped spliced beams

5.2. Bearing Capacity and Ductility of Specimens

After processing and analyzing the test data of four groups of specimens, the bearing capacity and ductility coefficient of four specimens were obtained. See Table 3.

Table 3. Bearing capacity and ductility coefficient of specimens

specimen number	equivalent yield state		limiting condition		collapse state		displacement ductility factor
	P_y/kN	Δ_y / mm	P_{max} /kN	Δ_{max} / mm	P_u/kN	Δ_u / mm	$\mu = \Delta u/\Delta y$
III-A	30.12	3.56	35.65	5.54	31.46	6.75	1.85
III-B	27.69	3.75	31.97	5.69	28.43	6.96	1.86
III-C	43.75	3.58	47.89	5.52	40.88	6.02	1.68
III-D	38.89	3.78	43.26	5.89	39.56	6.15	1.63

It can be seen from the table that the equivalent yield strength and ultimate yield load of III-A test components are larger than those of III-B test components, and there is little difference in ductility coefficient. The equivalent yield load and ultimate yield load of III-D are both smaller than III-C, and the ductility coefficient is similar. The equivalent yield load and ultimate yield load of III-D and III-C are higher than III-A and III-B, and the ductility coefficient of III-D and III-C is weaker than III-A and III-B. It can be concluded that the mechanical properties of i-shaped section are better than those of box-shaped section. The mechanical properties of the components with dense self-tapping screw spacing are better than those with small self-tapping screw spacing.

6. Numerical Analysis

6.1. Establishment of Finite Element Model

Because the plate thickness of cold-formed thin-walled steel is relatively small, Shell181 shell unit in ANSYS is used to simulate cold-formed thin-walled C member and stiffener in the test. At the same time, the pad at the loading point is also simulated by it. Shell181 unit has 4 main nodes, each of which has 6 degrees of freedom. Shell shell unit is planar quadrilateral, as shown in FIG. 7. This shell element is suitable for all kinds of thin-walled test objects, so it is also suitable for the numerical simulation of cold-formed thin-walled steel beam test. The model is established according to the bottom-up method: firstly, the key points of the finite element numerical analysis model of the double spliced cold-formed thin-walled steel beam are created, and then the points are connected into lines, and then the surfaces are generated through the connected lines, and finally the graphs are formed. The model is established by using the mirror

ISSN: 2688-8653

function in ANSYS, a quarter model is established at the beginning of the cold formed thin-wall steel beam model, and then the complete model is generated by using the mirror function. FIG. 8 shows the establishment of the geometric model of the segmented cold-formed thin-wall steel beam.

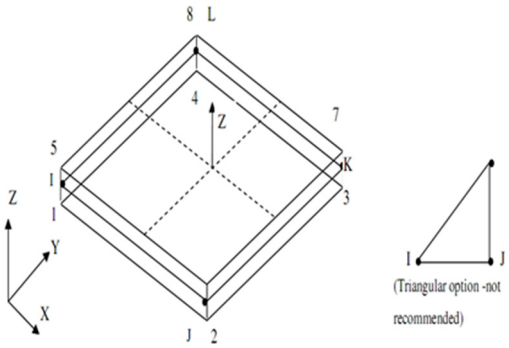

Figure 7. Geometric model of Shell 181 unit

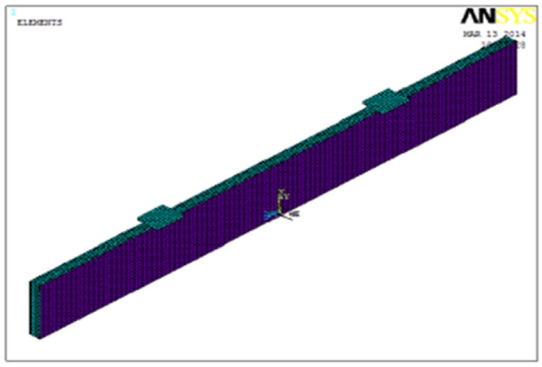

Figure 8. Geometrical model of segmented cold-formed thin-walled steel beam

6.2. Finite Element Simulation Results

After the finite element simulation, the deformation diagram, displacement cloud diagram and stress cloud diagram of the test component are extracted. The deformation diagram, displacement cloud diagram and stress cloud diagram of the test component when local buckling occurs can be obtained through analysis, and the local buckling load of the test component when local buckling occurs can be calculated. Finite element analysis results of some test components are shown in FIG. 9.

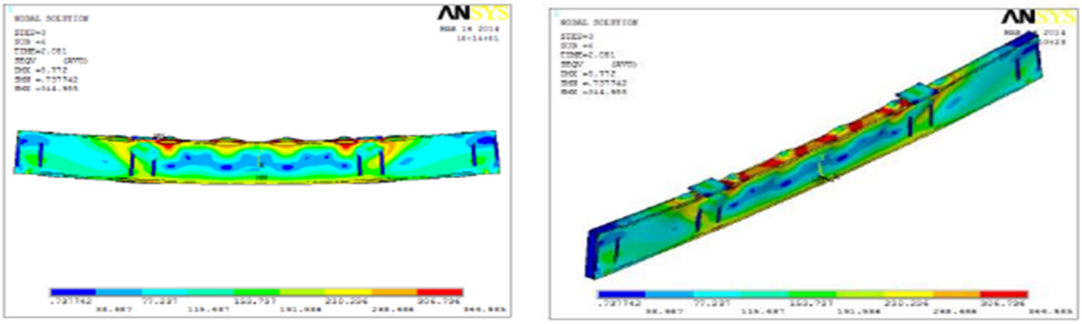

(a) Mises stress pattern at ultimate load (b) Mises stress pattern at ultimate load

Figure 9. Finite element analysis results of some test components

ISSN: 2688-8653

After the finite element numerical simulation is completed, the equivalent yield stress and ultimate bearing capacity of test components are extracted from the calculation results, as shown in Table 4. And through the two obtained specific numerical comparison.

Table 4. Comparison of bearing capacity of specimens

Specimen number	Equivalent yield capacity			ultimate bearing capacity			the relative ratio	
	experimnt P_y^t / kN	Finite element P_y^c / kN	P_y^c / P_y^t	experiment P_m^t / kN	Finite element P_m^c / kN	P_m^c / P_m^t	P_y^t / P_m^t	P_y^c / P_m^c
III-A	30.12	32.57	1.082	35.65	37.59	1.054	0.845	0.866
III-B	27.69	30.38	1.097	31.97	33.98	1.063	0.866	0.894
III-C	43.75	48.59	1.249	47.89	51.24	1.070	0.914	0.948
III-D	38.89	43.35	1.115	43.26	46.17	1.063	0.899	0.939

By analyzing and comparing the experimental results in the table, the equivalent displacement ductility coefficients of the four groups of test components were calculated and compared with the actual test results, as shown in Table 5.

Table 5. Comparison of equivalent ductility coefficients of specimens

Specimen number	Equivalent yield state		ultimate state		collapse state		Equivalent displacementductilit-y coefficient	Compare With-experimental results	
	Py/kN	Δ_y / mm	P_m / kN	Δ_m / mm	P_u / kN	Δ_u / mm	$\mu^c = \Delta_u / \Delta_y$	μ^t	$\frac{\mu_c}{\mu^t}$
III-A	32.57	4.32	37.59	6.15	32.64	8.24		1.85	1.03
III-B	30.38	4.58	33.98	7.22	29.53	8.57	1.87	1.86	1.01
III-C	48.59	4.36	51.24	6.89	41.75	8.78	2.01	1.68	1.20
III-D	43.35	4.19	46.17	7.24	40.89	9.15	2.18	1.63	1.34

7. Conclusion

Taking the assembling mode of large-section cold-formed thin-wall steel beam and the spacing of tapping screws as two main parameters, the bending tests and numerical analysis of four groups of members are carried out, and the following results are obtained:

(1)The bearing capacity of the test member can be improved by reducing the spacing of tapping screws. The ultimate bearing capacity of test specimen III-A is 10.3% higher than iiI-B, and the ultimate bearing capacity of numerical simulation is 9.6% higher than III-B. The ultimate bearing capacity of specimen III-C is 9.7% higher than iiI-D, and the numerical simulation results show that the ultimate bearing capacity of specimen III-C is 9.9% higher than III-D.

(2) The equivalent displacement ductility coefficients of i-shaped splice beams are slightly lower than those of box splice beams when the splice modes are the same.

(3) The ultimate bearing capacity of i-shaped spliced beams is higher than that of box-shaped spliced beams. By comparing the test results and numerical simulation results of specimen III-A and III-C, it can be seen that the ultimate bearing capacity of i-split specimen III-C is 25.6% higher than iiI-A, and the numerical simulation results show that the ultimate bearing capacity

ISSN: 2688-8653

of specimen III-C is 37.6% higher than III-A. The ultimate bearing capacity of specimen III-D is 26.1% higher than iiI-B.

(4) The failure of large section cold formed thin-wall steel spliced beams is caused by the increase of local buckling.

References

[1] Wang Haiming, Zhang Yaochun. Research on in-plane stability of c-section flexural members of cold-formed steel [J]. Building structure,2009,39(4):87-91.

[2] XU L, ZHOU X H, YUAN X L et al. On North A-merican and Chinese Standards for Design of Cold-formed Steel C-section Flexural Members[J]. Journal of Architecture and Civil Engineering, 2014, 31(1):16-35.

[3] Wu sheng, zhang sumei. Research on performance of a new type of section flexural member with cold-formed flange closure [J]. Industrial construction,2007,37(5):88-93.

[4] Wu Sheng, Zhang Sumei. Study on Mechanical Properties of New Type Cold-formed Box Composite Section Flexural Members [J]. Industrial construction,2008,38(2):91-95.

[5] Zhou Xuhong, Wang Shiji. Stability Theory and Application of Thin-walled Components [M]. Beijing: Science Press, 2009.

[6] Shi Yu, Zhou Xuhong, Yuan Xiaoli et al. Effective Width Method for Ultimate Bearing Capacity Calculation of Cold-formed Thin-wall Rolled Edge Channel Steel Composite I-Beam [J]. China civil engineering journal, 2011,44(6):8-17.

[7] Shi Yu, Zhou Xuhong, Nie Shaofeng et al. Reduction Strength Method for Ultimate Bearing Capacity Calculation of Cold-formed Thin-wall Winding Channel Composite I-Beam [J]. Engineering mechanics,2011,28(9):174-182.

[8] Chen Shaofan, Hui Ying. Correlation of Local Buckling of Cold-formed Steel and Effective Width of Flanged Plate [J]. Journal of xi 'an university of architecture and technology,1995,27(1):1-7.

[9] Shi Yu, Zhou Xuhong, Nie Shaofeng et al. Reduction Strength Method for Ultimate Bearing Capacity Calculation of Cold-formed Thin-wall Winding Channel Composite I-Beam [J]. Engineering mechanics,2011,28(9):174-182.

[10] Zhang Yaochun, Wang Haiming. Journal of building structures,2009,30(3):38-43.